PROCEEDINGS OF SCIENCE

Multiboson Production and Polarisation Measurements With the ATLAS Detector

Muhammad Alhroob[†,*]

The University of Warwick,
CV4 7AL, Coventry, UK

E-mail: muhammad.alhroob@cern.ch

Measurements of multiboson production at the LHC are important probes of the electroweak gauge structure of the Standard Model and can constrain anomalous gauge boson couplings. In these proceedings, measurements of triboson productions, $WZ\gamma$ and $W\gamma\gamma$ channels, by the ATLAS experiment at the LHC using 13 TeV dataset are reported. The measurement of ZZ production cross-sections using 13.6 TeV dataset is also presented. Studies of gauge-boson polarisation and their correlation with ZZ and WZ events are also presented. In WZ events, these studies have been extended to a phase space with high transverse momentum Z bosons.

ATL-PHYS-PROC-2024-071
24 September 2024

42nd International Conference on High Energy Physics (ICHEP2024)
18-24 July 2024
Prague, Czech Republic

[*]Speaker
[†]On behalf of the ATLAS Collaboration

© Copyright owned by the author(s) under the terms of the Creative Commons Attribution-NonCommercial-NoDerivatives 4.0 International License (CC BY-NC-ND 4.0).

1. Introduction

The ATLAS collaboration [1] at the LHC investigates multiboson productions, which provides crucial tests of the electroweak sector within the Standard Model (SM). These processes offer a unique probe of the non-Abelian structure through triple and quartic gauge couplings. Deviations from SM predictions could signal new physics. Multiboson measurements also constrain anomalous quartic gauge couplings using Effective Field Theory and resonant searches, imposing stringent limits on SM extensions. The longitudinal polarisation of vector bosons is emphasised as a key probe of Electroweak Symmetry Breaking (EWSB), being sensitive to new physics and a step toward vector-boson scattering measurements essential to understanding electroweak interactions.

2. Observation of $WZ\gamma$ production process

The ATLAS collaboration searched for the $WZ\gamma$ production process using the full Run-2 dataset, with an integrated luminosity ($\mathcal{L}$) of 140 fb^{-1} [2]. Events were required to have three leptons (electrons or muons) with transverse momentum $p_{\mathrm{T}} > 30$ for the leading lepton and > 20 GeV for the subleading leptons, respectively. The lepton pair originating from the Z boson decay was required to have an invariant mass $m_{\ell\ell} > 80$ GeV, and events had to include missing transverse momentum $E_{\mathrm{T}}^{\mathrm{miss}} > 20$ GeV. Additionally, a well-isolated photon with $p_{\mathrm{T}} > 15$ GeV was required.

A data-driven "Fake Factor" method was employed to estimate the non-prompt background contributions, when misidentified jets or non-prompt leptons mimic the signal's photon or lepton signatures. The WZ, ZZ, $Z\gamma$ and $t\bar{t}\gamma$ are the dominant processes in the non-prompt lepton background. In contrast, background with prompt leptons, such as $ZZ\gamma$, was estimated using Monte Carlo simulations. Figure 1a and Figure 1b show good agreement between the data and the post-fit signal and background predictions for the photon p_{T}^{γ} and $m_{\ell\ell}$ distributions, respectively.

A profile-likelihood fit was used to extract the signal and two background normalisation factors: ZZ and $ZZ\gamma$. The significance of the observed signal was 6.3σ, compared to an expected 5.0σ significance. The results agreed with SM predictions within 1.5σ. The measured fiducial cross section was 2.01 ± 0.30 (stat.) $\pm$ 0.16 (syst.) fb. The dominant systematic uncertainties in this measurement were related to photon identification and isolation.

3. Observation of $W\gamma\gamma$ production process

The ATLAS collaboration searched for the $W\gamma\gamma$ production process using the full Run-2 dataset [3], which is sensitive to the $WW\gamma\gamma$ and $WW\gamma$ gauge couplings and plays a crucial role in testing the electroweak sector of the SM. Additionally, it serves as an important background for Higgs boson processes, particularly $WH \to W\gamma\gamma$.

Events were required to have two isolated photons with $p_{\mathrm{T}} > 20$ GeV, an isolated electron or muon with $p_{\mathrm{T}} > 25$ GeV and $E_{\mathrm{T}}^{\mathrm{miss}} > 25$ GeV. Furthermore, the transverse mass of the W boson $m_{\mathrm{T}}^{W} = \sqrt{2p_{\mathrm{T}}^{\ell}E_{\mathrm{T}}^{\mathrm{miss}}\,(1 - \cos\Delta\phi)}$ was required to be greater than 40 GeV, where $\Delta\phi$ is the difference in azimuthal angles between the lepton momentum and missing transverse momentum. Additional requirements were applied to reduce the $Z\gamma$ background events. Events were required to have $m_{\ell\gamma\gamma}$, $m_{\ell\gamma_1}$ and $m_{\ell\gamma_2} \notin [82, 100]$ GeV, where γ_1 and γ_2 are the leading and subleading photons. The p_{T} of the $\ell\ell\gamma$ system was also required greater than 30 GeV.

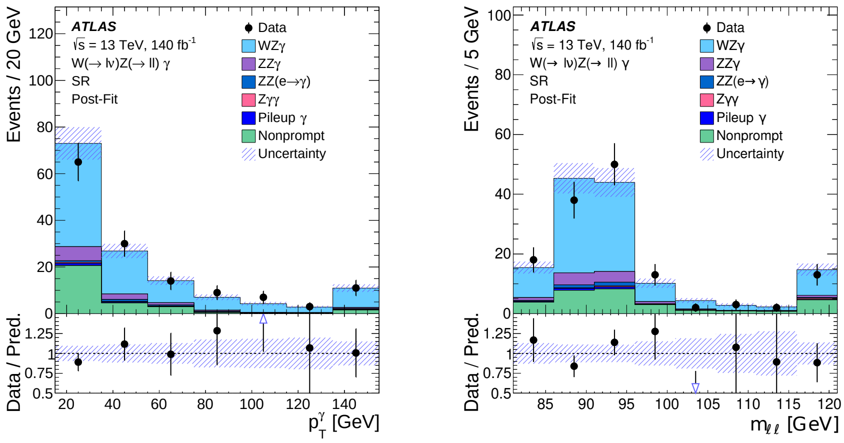

(a) **(b)**

Figure 1: (a) The photon p_{T}^{γ} distribution is the signal region (SR) [2]. (b) The $m_{\ell\ell}$ distribution in the SR [2].

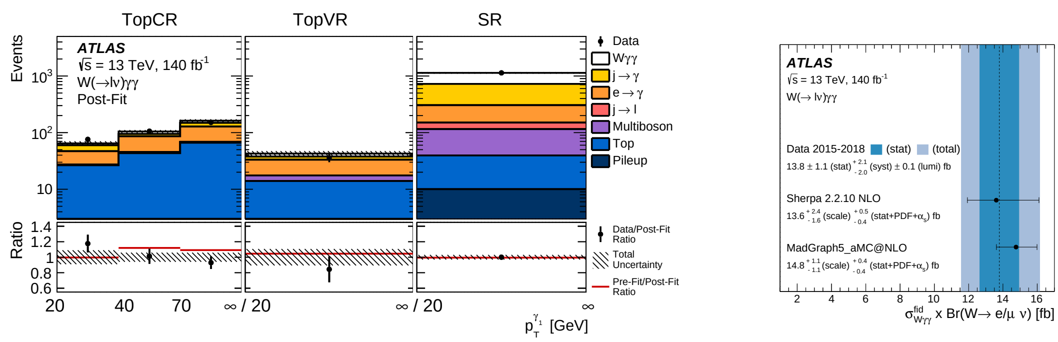

(a) **(b)**

Figure 2: (a) Comparison of data and predicted yields in the TopCR as a function of leading photon p_{T}, and for the TopVR region and SR, each as a single bin [3]. (b) Measured fiducial $(W \to e\nu/\mu\nu)\gamma\gamma$ cross section compared with two MC generator predictions [3].

A data-driven method was used to estimate non-prompt background contributions where misidentified jets or neutral hadron decays mimicked signal photons ($j \to \gamma$). A similar approach was used for estimating electrons faking photons or hadronic jets promoting fake leptons. Conversely, backgrounds with prompt photons and leptons, such as $t\bar{t}\gamma$, were estimated using MC simulations, with normalisation controlled with the Top Control region (TopCR) and validated in the independent top validation region (TopVR). Figure 2a shows the yields for the signal, TopCR, and TopVR, demonstrating a good agreement between the data and the predictions.

A profile-likelihood fit was performed on the signal region and a top-quark control region to extract the signal and constrain the top-quark background normalisation. The observed and expected signal significance was 5.6σ. The measured fiducial cross section was $\sigma_{\mathrm{fid.}} = 13.8 \pm 1.1$ (stat.) $^{+2.1}_{-2.0}$ (sys.) ± 1.1 (lumi.) fb, with a relative uncertainty of 17%, and is presented in Figure 2b. The dominant systematic uncertainty originated from the jet $\to \gamma$ background estimation.

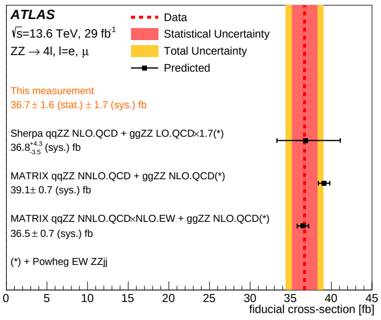

(a)

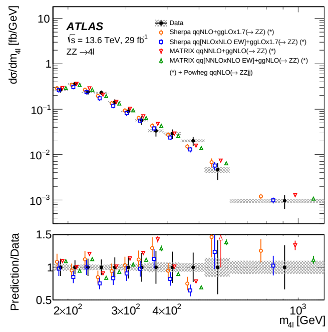

(b)

Figure 3: (a) The measured fiducial cross section compared with the predictions from MC simulations [4]. (b) The measured differential cross-sections compared with the predictions in $m_{4\ell}$ [4].

4. Measurement of ZZ production cross-sections at $\sqrt{s} = 13.6$ TeV

The ATLAS collaboration searched for the ZZ pairs production using a partial Run-3 dataset corresponding to $\mathcal{L} = 29$ fb^{-1} [4]. The ZZ is crucial process for probing anomalous neutral triple gauge couplings (aTGCs) and studying off-shell Higgs boson production. The fiducial cross section was measured in events with a 4ℓ final state, requiring four isolated leptons (electrons or muons). The leading lepton had to satisfy $p_T > 27$ GeV, and subleading leptons required to have $p_T > 10$ GeV. Two Z-boson were reconstructed from lepton pairs and required to have $66 < m_{\ell\ell} < 116$ GeV, and the invariant mass of the four-lepton system, $m_{4\ell}$, had greater than 180 GeV.

A single bin was used to extract the fiducial cross section, extrapolated to the total cross section for $66 < m_{\ell\ell} < 116$ GeV for both Z bosons. The fiducial cross section was $\sigma_{\text{fid.}} = 36.7 \pm 1.6$ (stat.) ± 1.5 (sys.) ± 0.8 (lumi.) fb, shown in Figure 3a. The total cross section, $\sigma_{\text{tot.}} = 16.8 \pm 0.7$ (stat.) ± 0.7 (sys.) ± 0.4 (lumi.) pb, was consistent with SM predictions. An iterative Bayesian unfolding [5] was used to extract the differential cross sections for $m_{4\ell}$ and $p_T(4\ell)$ kinematic variables, and was found to agree with SM predictions, as shown in Figure 3b.

5. ZZ polarisation and CP results

Using the full Run-2 data, the ATLAS collaboration measured the longitudinal polarisation of Z bosons ($Z_L Z_L$) using the $ZZ \to 4\ell$ final state [6]. The polarisation measurements of massive electroweak bosons provide direct insights into the EWSB mechanism and are sensitive to BSM physics.

A Boosted Decision Tree (BDT) was trained to distinguish the $Z_L Z_L$ state from the $Z_L Z_T$ and $Z_T Z_T$ polarisation states. Figure 4a presents the post-fit BTD distribution in the signal region. A profile likelihood fit was performed on the BDT distribution to extract the polarisation components. The production of two longitudinally polarised Z bosons ($Z_L Z_L$) was measured with a significance of 4.3σ, compared to the expected significance of 3.8σ. The measured fiducial cross section was $\sigma_{\text{fid.}} = 2.45 \pm 0.60$ fb, consistent with the SM prediction. The measurement was statistically limited, and interference effects and theoretical modelling were the largest systematic uncertainties.

The CP properties of the ZZ system was studied using CP-sensitive observable. A CP-odd Optimal Observable (OO) was defined, combining the CP-sensitive polar and azimuthal angles of

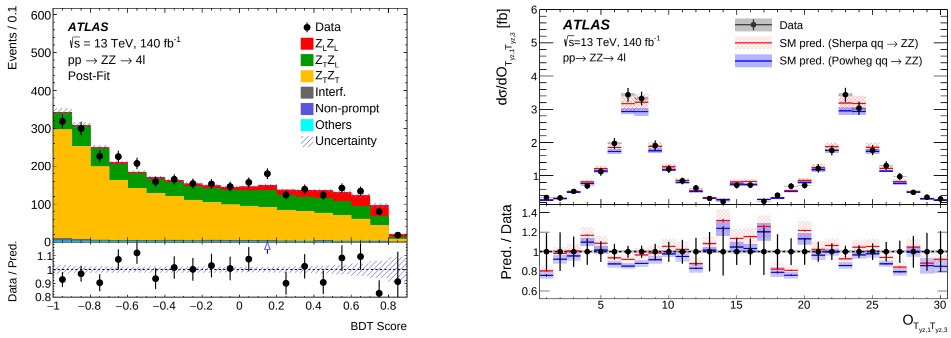

(a) **(b)**

Figure 4: (a) The BDT distribution of the data and the post-fit SM predictions [6]. (b) Unfolded differential cross section as a function of the flattened OO distribution [6]

both Z-boson systems, $T_{\text{yz},1(3)} = \sin(\phi_{1(3)}) \times \cos(\theta_{1(3)})$, with the polar angles θ_1 and θ_3 for the Z_1 and Z_2 bosons, respectively, and the azimuthal angles ϕ_1 and ϕ_3, reconstructed in a reference frame designed to measure the Z-boson spins. The two-dimensional differential cross section for the CP-odd sensitive variable, $T_{\text{yz},1}$ versus $T_{\text{yz},3}$, is symmetric in the SM but asymmetric in the presence of CP-odd anomalous neutral triple gauge couplings (aNTGC). The OO distribution was flattened, unfolded as shown in Figure 4b, and used to set exclusion limits at 95% confidence level on the effective vertex function parameterised by two coupling parameters, f_γ^4 and f_Z^4.

6. Energy Dependence of Diboson Polarisation and Radiation-Amplitude-Zero Effect in WZ Production

Using the Run-2 pp dataset, the ATLAS collaboration conducted the first study of the energy dependence of WZ joint-polarisation states, the longitudinal-longitudinal (W_0Z_0) and other polarisation states: W_0Z_T, $W_\text{T}Z_0$, and $W_\text{T}Z_\text{T}$ [7]. Polarisation fractions were measured as a function of p_T^Z for two ranges: 100-200 GeV and above 200 GeV, providing insight into the behaviour across different energy scales.

A BDT was trained for each p_T^Z region to distinguish the W_0Z_0 component from other polarisation states. Two profile-likelihood fit approaches were performed to extract the polarisation fractions. In the first approach, three free parameters were used for each p_T^Z region, resulting in a 5.2σ observation of the W_0Z_0 state in the $100 < p_\text{T}^Z < 200$ GeV range, compared to the expected significance of 4.3σ. However, in the $p_\text{T}^Z > 200$ GeV region, the observed significance was 1.6σ compared to the expected significance 2.5σ. In the second scenario, where only two free parameters were considered, the observed significance for the $100 < p_\text{T}^Z < 200$ GeV range increased to 7.7σ compared to an expected significance of 6.9σ, while in the $p_\text{T}^Z > 200$ GeV range, the observed significance increased to 3.2σ, compared to an expected significance of 4.2σ. The leading systematic uncertainty came from higher-order QCD effects.

At leading-order QCD, the cross section for the $W_\text{T}Z_\text{T}$ polarisation state drops to zero when the scattering angle θ_v approaches $\pi/2$. Here, θ_v is the scattering angle of the W boson in the WZ rest frame relative to the direction of the incoming antiquark. This phenomenon is known as the Radiation Amplitude Zero (RAZ) effect, a direct consequence of the gauge structure of the SM.

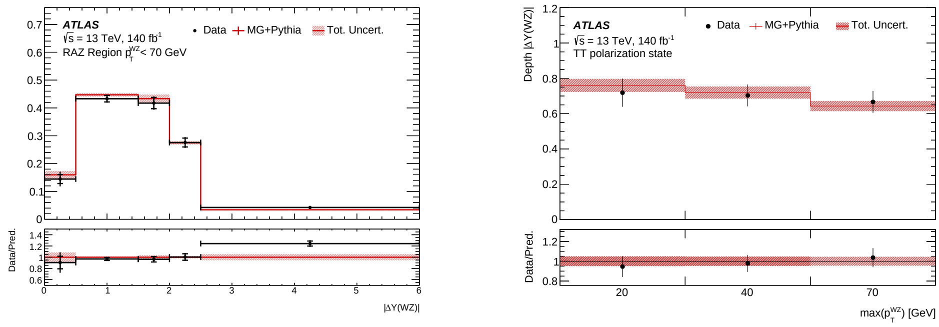

(a) **(b)**

Figure 5: (a) Comparison between the $00 + 0T + T0$-subtracted normalised unfolded $|\Delta Y(WZ)|$ distribution for TT events with $p_{\mathrm{T}}^{WZ} < 70$ GeV [7]. (b) The RAZ dip in three p_{T}^{WZ} ranges, calculated using the unfolded $|\Delta Y(WZ)|$ distribution of the TT polarisation [7].

The RAZ effect is pronounced in the $\Delta Y(WZ)$ and $\Delta Y(\ell_W Z)$ distributions, where ℓ_{W} is the lepton coming from the W boson decay, and Δy is the difference in rapidity. However, the effect can be smeared by higher-order QCD corrections, e.g. events with high p_{T}^{WZ}.

To quantify the dip in the ΔY distribution, the depth variable was introduced, defined as $D = 1 - 2\frac{N(|\Delta Y|<0.5)}{N(0.5<|\Delta Y|<1.5)}$, where N is the number of events extracted from the unfolded distribution. A positive D indicates the existence of a dip. The D was calculated for both the $\Delta Y(WZ)$ and $\Delta Y(\ell_{\mathrm{W}} Z)$ distributions in different p_{T}^{WZ} ranges, such as $p_{\mathrm{T}}^{WZ} < 20$ GeV, $p_{\mathrm{T}}^{WZ} < 40$ GeV, and $p_{\mathrm{T}}^{WZ} < 70$ GeV, to explore how the RAZ effect is reduced with higher-order QCD corrections. Figure 5a shows a comparison between the unfolded $\Delta Y(WZ)$ distribution and the TT-only SM prediction for events with $p_{\mathrm{T}}^{WZ} < 70$ GeV. Figure 5b shows the measured and predicted D values using the $|\Delta Y(WZ)|$ distribution for three p_{T}^{WZ} ranges.

7. Summary

Using the full Run-2 dataset, the ATLAS collaboration observed $WZ\gamma$ and $W\gamma\gamma$ production processes with 6.3σ and 5.6σ significance, respectively. The ZZ fiducial cross section was measured with the partial Run-3 dataset and extrapolated to the total cross section. The ZZ longitudinal polarisation was measured with 4.3σ significance, and CP properties were used to set limits on aNTGC. The WZ joint-polarisation was studied in two p_{T}^{Z} regions. The Radiation-Amplitude-Zero effect was confirmed providing a stringent test of the Standard Model.

References

[1] ATLAS Collaboration, *The ATLAS Experiment at the CERN Large Hadron Collider*, *JINST* **3** (2008) S08003.

[2] ATLAS Collaboration, *Observation of $WZ\gamma$ Production in pp Collisions at $\sqrt{s} = 13$ TeV with the ATLAS Detector*, *Phys. Rev. Lett.* **132** (2024) 021802 [2305.16994].

[3] ATLAS Collaboration, *Observation of $W\gamma\gamma$ triboson production in proton-proton collisions at $\sqrt{s} = 13$ TeV with the ATLAS detector*, *Phys. Lett. B* **848** (2024) 138400 [2308.03041].

[4] ATLAS Collaboration, *Measurement of ZZ production cross-sections in the four-lepton final state in pp collisions at* $\sqrt{s} = 13.6$ *TeV with the ATLAS experiment*, *Phys. Lett. B* **855** (2024) 138764 [2311.09715].

[5] G. D'Agostini, *A multidimensional unfolding method based on bayes' theorem*, *Nuclear Instruments and Methods in Physics Research Section A: Accelerators, Spectrometers, Detectors and Associated Equipment* **362** (1995) 487.

[6] ATLAS Collaboration, *Evidence of pair production of longitudinally polarised vector bosons and study of CP properties in* $ZZ \to 4\ell$ *events with the ATLAS detector at* $\sqrt{s} = 13$ *TeV*, *JHEP* **12** (2023) 107 [2310.04350].

[7] ATLAS Collaboration, *Studies of the Energy Dependence of Diboson Polarization Fractions and the Radiation-Amplitude-Zero Effect in WZ Production with the ATLAS Detector*, *Phys. Rev. Lett.* **133** (2024) 101802 [2402.16365].